Dyes and Pigments 172 (2020) 107838

Contents lists available at ScienceDirect

Dyes and Pigments

journal homepage: www.elsevier.com/locate/dyepig

Multipolar triphenylamines: Effect of spectator donor-acceptor pair on intramolecular charge transfer interactions

Pichandi Thamaraiselvi[a], Elumalai Varathan[a,b,c,d], Venkatesan Subramanian[a,b,c,**], Shanmugam Easwaramoorthi[a,b,c,*]

[a] Inorganic & Physical Chemistry Laboratory, CSIR-Central Leather Research Institute, Adyar, Chennai, 600020, India
[b] CSIR-Network of Institutes for Solar Energy, New Delhi, India
[c] Academy of Scientific and Innovative Research, New Delhi, India
[d] Department of Chemistry, Indian Institute of Technology Madras, Chennai, 600 036, India

ARTICLE INFO

Keywords:
Triphenylamine
Charge transfer
Donor-acceptor system
Solvatochromism
Symmetry broken dipolar CT

ABSTRACT

Donor (D) - Acceptor (A) compounds based on triphenylamine (TPA) substituted with cyano, nitro, and formyl functional groups were synthesized in dipolar (DA), quadrupolar (DA_2), and octupolar (DA_3) configurations and characterized using different spectral techniques. Bond-length alternation (BLA) values of the phenyl ring were found to be in the range between 0.012 and 0.022 Å, suggest the charge transfer occurs in the ground state itself, which in fact differs distinctly with respect to number of acceptor groups in the TPA core. Steady-state and time-resolved fluorescence studies indicates the existence of dipolar charge transfer interactions in all the molecules by the virtue of reducing their molecular symmetry. Interestingly, for dipolar molecule, the efficiency of ICT interactions is elucidated by the slope of the Lippert-Mataga plot which exhibits the linear relationship with the Hammett (σ) constant. Controlling the rotation of N–C bond of amino and phenylene moiety by lowering the surrounding temperature drastically affect the fluorescence and reveals that the structural changes at the excited state plays a crucial role in ICT processes. Notably, the mono-nitro substituted triphenylamine exhibits specific solvent-solute interactions exclusively with the chlorinated solvents at the excited state with the emission in NIR region and is tailing over 800 nm.

Introduction

Organized assemblies of chromophores held by covalent bonding, molecular aggregates, and light-harvesting pigment complexes in nature are always fascinating and these systems provide tremendous scope to unravel the excitation localization/delocalization, and subsequent energy or electron transfer processes. These processes are mainly influenced by the distance as well as the extent of electronic coupling with the chromophores. The excitation can be delocalized among the chromophores through space. There are instances where the chromophore is not an isolated molecular entity, but it is a part of the molecule, called as sub-chromophore, a situation often noted in molecules bearing multiple electron donating (donor(D)) and electron accepting (acceptor(A)) moieties bonded through $\pi-$conjugation. In this regard, the structural motifs shown in Scheme 1 such as quadrupolar, DAD [1–6] or ADA [7] and octupolar, DA_3 [8–11] or AD_3 [11,12] have attracted much attention due to the multitude of applications in organic electronics.

These molecules show large two-photon absorption coefficient [13–15], better efficiency as a sensitizer in dye-sensitized solar cells (DSSC) [16–18], organic photovoltaics, organic light emitting devices [19–21], and fluorescent probes for bio-imaging [22–24], when compared to the simplest dipolar D-A systems. Asymmetrical substituents in these molecules facilitate the intramolecular charge transfer (ICT) interactions and its efficiency has a significant influence on the associated electronic properties, which can conveniently be tuned by the judicious combination of electron donating or withdrawing moieties [22–28]. Nonetheless, the structure-property relationship with respect to ICT interactions with the two-photon absorption or efficiency of DSSC, hole transport property, is limited. Essentially, the difference between ICT interactions of quadrupolar and octupolar molecules with respect to simple dipolar motifs is due to the nature of charge transfer interactions. ICT state of quadrupolar and octupolar molecules might show net zero dipole moment change when all the donor and acceptor groups get

* Corresponding author. Inorganic & Physical Chemistry Laboratory, CSIR-Central Leather Research Institute, Adyar, Chennai, 600020, India.
** Corresponding author. Inorganic & Physical Chemistry Laboratory, CSIR-Central Leather Research Institute, Adyar, Chennai, 600020, India.
E-mail addresses: subbu@clri.res.in (V. Subramanian), moorthi@clri.res.in (S. Easwaramoorthi).

https://doi.org/10.1016/j.dyepig.2019.107838
Received 25 December 2018; Received in revised form 14 August 2019; Accepted 24 August 2019
Available online 28 August 2019
0143-7208/

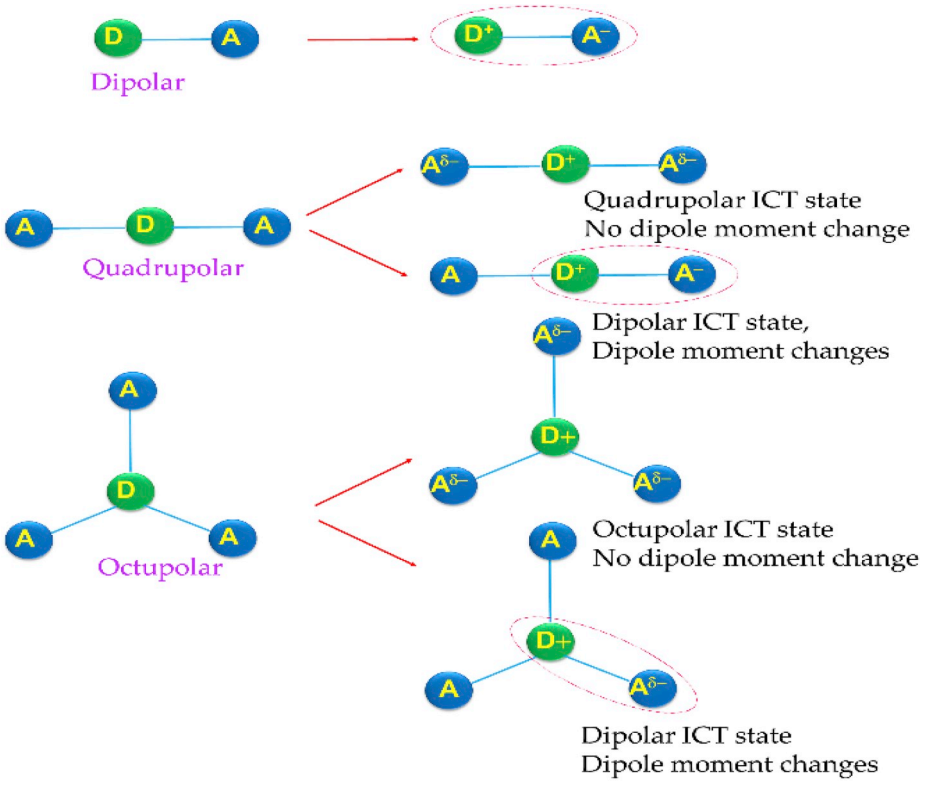

Scheme 1. Structure of the triphenylamine based donor-acceptor compounds.

involved in ICT state formation. On the other hand, the majority of quadrupolar and octupolar molecules exhibit a change in dipole moment, which is evident from the solvent polarity induced red shifted fluorescence. This feature reveals that though the quadrupolar and octupolar compounds have more than one donor-acceptor pairs, the ICT state is formed by one of the pairs and the remaining donors or acceptors are not involved in the ICT state formation. Thus, the original symmetry of the chromophores is reduced to the lowest symmetry, and this process is driven by the local field generated by the solvents and/or the structural fluctuations. Notably, symmetry broken ICT states leave some donor/acceptor moieties as a spectator and this spectator pair is expected to influence ICT state significantly. Further, the real-time observation of symmetry breaking is limited despite several femtosecond transient absorption studies. However, recently, Vauthey et al. [29] used femtosecond transient infrared spectroscopy to unravel the process. It has been demonstrated that the nature of the relaxed singlet excited state of the quadrupolar molecule is symmetric in nonpolar solvents whereas in the polar media symmetry broken state with one arm bears more excitation than the other is formed; it is purely a dipolar state with the localized excitation. However, several intriguing issues need to be explored to develop the reasonable understanding of these processes and their implications in the development of devices.

To unravel the nature of ICT interactions in multiple D-A molecules, in this work, we have developed dipolar, quadrupolar, and octupolar molecules using triphenylamine (TPA) moiety as donor and nitro, aldehyde, and cyano groups as acceptors. It is important to note that the core structure and shape of the molecule remain identical, which is one of the crucial factors in determining the two-photon absorption efficiency [30]. Detailed photophysical studies have been carried out to understand the ICT interactions of various D-A chromophores, which suggest that though all of them form a dipolar charge transferred states, still the excited state is unique concerning the number of acceptor substituents.

Results and discussion

Mono-, di-, and tri-substituted triphenylamine derivatives with electron withdrawing nitro (**NO_2**), formyl (**CHO**), and cyano (**CN**) groups at the para-phenylene position shown in Chart 1 were synthesized by following literature methods [31,32]. Briefly, the nitro derivatives, 4-nitro-N,N-diphenylaniline (**mNO_2**), 4-nitro-N-(4-nitrophenyl)-N-phenylaniline (**dNO_2**), and tris(4-nitrophenyl) amine (**tNO_2**) were synthesized in moderate yields by nitration reaction using different equivalents of copper nitrate and acetic anhydride. Vilsmeier-Haack reaction of triphenylamine with different equivalents of $POCl_3$/DMF as shown in Scheme S1 (SI) affords 4-(diphenylamino) benzaldehyde (**mCHO**), 4,4'- (phenylazanediyl) dibenzaldehyde (**dCHO**), 4,4′,4″-nitrilotribenzaldehyde (**tCHO**) in quantitative yields. Synthesis of cyano derivatives 4-(diphenylamino) benzonitrile (**mCN**), 4,4'-(phenylazanediyl) dibenzonitrile (**dCN**), and 4,4′,4″-nitrilotribenzonitrile (**tCN**) was reported previously [11]. All the compounds were characterized thoroughly using ^1H, ^{13}C NMR, and FTIR techniques.

The structures of **mNO_2**, **mCN**, and **tCN** were also determined by single crystal X-ray diffraction method (SI, Table S1). It can be seen from Fig. 1 that all the TPA derivatives exhibit propeller-like structure.

It has been known that molecules having both electron rich and poor moieties would be the combinations of neutral and charge separated canonical forms, which can be identified by comparing the degree of bond-length alternations, δr within the phenyl ring. For example, δr-value calculated using equation (1) corresponds to 0 and 0.08–0.10 Å respectively for benzene and quinonoid forms. The bond lengths a, a', b, b', c, c' denoted in the single crystal X-ray structure of the compounds given in Fig. 1 were used to calculate the δr-value for TPA derivatives [33–36].

$$\delta r = \left\{\frac{(a + a')}{2} - \frac{(b + b')}{2}\right\} + \left\{\frac{(c + c')}{2} - \frac{(b + b')}{2}\right\} \quad (1)$$

The geometrical parameters calculated at B3LYP/6-31 + G* level of theory using Gaussian 09 were used for the compounds [37], which do

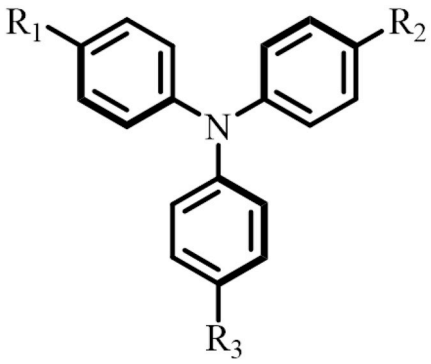

	R_1	R_2	R_3
mNO_2	NO_2	H	H
dNO_2	NO_2	NO_2	H
tNO_2	NO_2	NO_2	NO_2
mCHO	CHO	H	H
dCHO	CHO	CHO	H
tCHO	CHO	CHO	CHO
mCN	CN	H	H
dCN	CN	CN	H
tCN	CN	CN	CN

Chart 1. Structure of TPA substituted with various acceptor groups.

not have crystal structures to calculate the δr-value. The experimental and theoretical δr values summarized in Table 1 indicates that the values obtained from computational methods appear to be overestimated by the factor of 0.65 ± 0.1 when compared to the single crystal X-ray structure values. Since same methodology has been adopted to obtain δr for all the molecules, it is reasonable to use the computed δr for rationalizing the ground-state charge transfer character. The nonzero δr value as presented in Table 1 for all the TPA derivatives indicates the presence of substantial charge transfer character. Specifically, δr value of 0.021, 0.019, and 0.012 Å, respectively for **mCN**, **dCN**, and **tCN** indicates the significant quinonoid contribution to the phenyl rings in the ground state. Though generalization of δr with respect to number of substituents has not been arrived, δr values in all the cases follow mono- > di- > tri-substituted derivatives, which underscores that the quinonoid contribution is more for monosubstituted compounds which can be used as a scale to define the strength of charge transfer interactions.

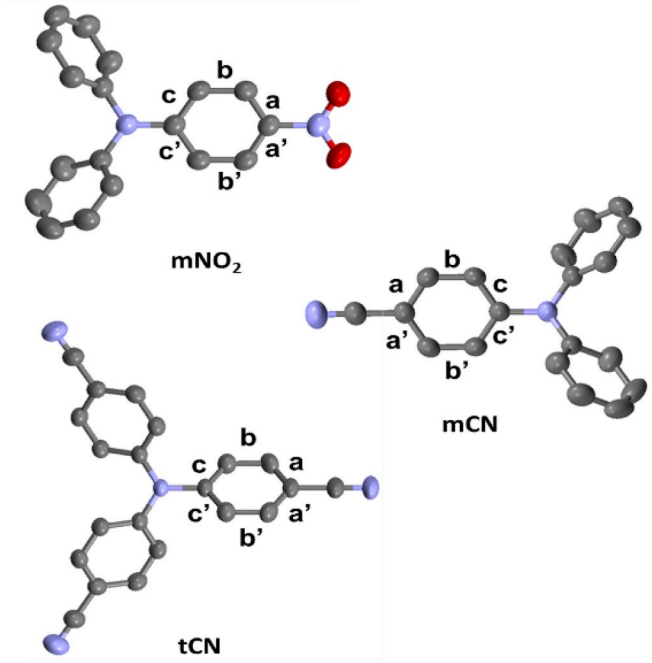

Fig. 1. Single crystal X-ray structures of **mNO_2**, **mCN** and **tCN** (hydrogen atoms are omitted for clarity).

The UV–visible absorption and fluorescence spectra measured in toluene exhibits intense transitions in the UV region as shown in Fig. 2, which is characteristic to the nature of the substituent. It is evident from the spectra that the lowest energy absorption observed at 400, 359, 330 nm in toluene for **mNO_2**, **mCHO** and **mCN**, respectively are according to their Hammett σ constants [38] where the strongest electron withdrawing group red-shifts the absorption to the maximum extent. Additional substitution resulted in spectral shifts along with the further intensification of lowest energy absorption bands (Tables S2 and S3 and Figs. S1 and SI). The data clearly specifies that, the lowest energy absorption is dominated by HOMO→ LUMO transition for all the molecules, while next higher energy transitions are distinctly different for mono, di, and tri-substituents. Specifically, DA_2 molecules show two well-resolved absorption bands because of the occurrence of HOMO→ LUMO + 1 transition at the wavelengths which are blue shifted by 45, 41, and 33 nm for nitro, formyl, and cyano substituents, respectively. On the other hand, the tri-substituted DA_3 molecules exhibit absorption maximum with increased oscillator strength by the factor of two, when compared to their respective mono congener. Indeed, octupolar derivatives have two isoenergetic transitions with nearly identical oscillator strength originated from HOMO→LUMO and HOMO→LUMO + 1 transitions, which can also be noticed from the nearly two times of molar

Table 1
Summary of the selected structural parameters such as bond lengths, bond angles from single crystal X-ray data and theoretical calculation torsion angle and chemical shift values of proton NMR.

Cpd	δr_{exp}[Å]	δr_{cal}[Å]	θ_{exp}[a] [deg]	θ_{cal}[b] [deg]
mNO_2	0.013	0.023	44.0	48
dNO_2	–	0.022	–	33
tNO_2	–	0.013	–	40
mCHO	–	0.022	–	47
dCHO	–	0.018	–	35
tCHO	–	0.015	–	40
mCN	0.013	0.021	37.0	48
dCN	–	0.019	–	38
tCN	0.009	0.012	30.4	41
TPA	−0.013	0.007	49.9	41

[a] The torsion angle between acceptor moiety and donor rings determined from the crystal structure.
[b] The torsion angle determined by theoretical calculation.

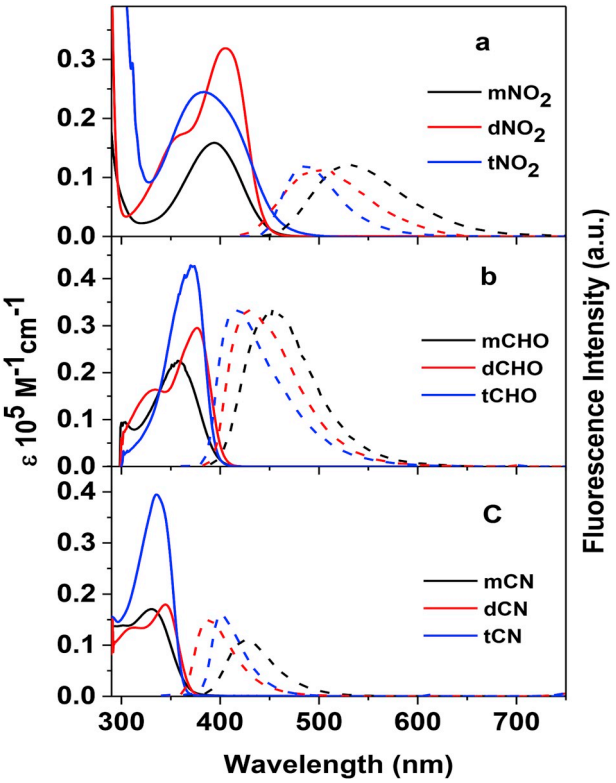

Fig. 2. UV–visible absorption (solid line) and fluorescence spectra (dotted line) of a) nitro, b) aldehyde and c) cyano substituted TPA derivatives in toluene.

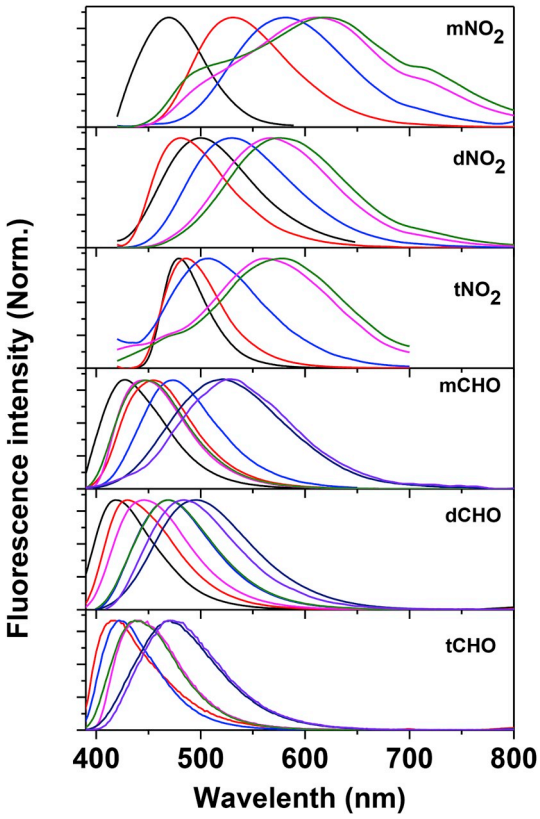

Fig. 3. Fluorescence spectra of **mNO_2**, **dNO_2**, **tNO_2** and **mCHO**, **dCHO**, **tCHO** in different solvents: Hexane (Black line), Toluene (red), Ethyl Acetate (blue), Chloroform (Magenta), Dichloromethane (Olive), Acetonitrile (Navy), Dimethylsulfoxide (Violet). (For interpretation of the references to colour in this figure legend, the reader is referred to the Web version of this article.)

extinction coefficient values in experimental absorption spectra with respect to their corresponding mono-substituted ones.

The measured fluorescence spectrum of all the investigated molecules are shown in Fig. 2 and Tables S4–S6 (SI). The emission maximum of the compounds **mNO_2**, **dNO_2**, **tNO_2**, **mCHO**, **dCHO**, **tCHO**, **mCN**, **dCN,** and **tCN** in toluene solvent are observed at 530, 481, 487, 455, 430, 417, 405, 387 and 369 nm respectively. In all the cases, mono-substituted TPA's show red-shifted fluorescence combined with larger Stokes shift values of 17251, 15400, 6401 cm^{-1} respectively for **mNO_2**, **mCN**, and **mCHO**. The larger Stokes shift value, an indication for the notable structural difference between the ground and excited states of the molecule would have originated from the intramolecular charge transfer interactions and were further probed by the solvent polarity induced fluorescence spectral studies.

Fig. 3 depicts the fluorescence spectra of nitro and formyl substituted TPA's in solvents of different polarity and in fact all the derivatives exhibit gradually red-shifted fluorescence, however to different extent while going from non-polar, toluene to polar, acetonitrile solvent. Notably, the magnitude of the red-shifted fluorescence maximum follows DA > DA_2 > DA_3 configuration and the quantification in terms of Lippert-Mataga plot i.e. Stokes shift against the solvent polarity parameter (Figs. S2 and SI) yields the largest slope values for mono-substituted derivatives. This feature originated from the dipole moments changes upon excitation could be attributable to the formation of dipolar CT states. Notably, the DA_2 and DA_3 can have the option of forming quadrupolar, $D^+(A^{\delta-})_2$ and octupolar, $D^+(A^{\delta-})_3$ CT states, however with net zero dipole moment change identified by the non-solvatochromism in fluorescence. In the ground state of DA_2, the C_2 axis passing through the unsubstituted phenyl ring becomes negated when one of the two acceptor bears charge after excitation. Similarly, the C_3 symmetry axis of DA_3 is reduced to C_2 symmetry when one of the acceptor groups accepts the charge after photoexciation. Notably, the symmetry broken dipolar CT states involves only one of the sub-chromophoric part AD^+A^-/$A_2D^+A^-$ and the remaining pairs are mere spectators. It should also be noted that the silent spectator moieties would also have the equal chance to become part of the dipolar CT state. Hence, quadrupolar and octupolar derivatives might show two and three isoenergetic, inter-convertible, symmetry broken, dipolar CT states, respectively. Though no systematic relationship has been derived from the Lippert-Mataga plot, the higher slope value for mono-substituted derivatives than their respective di- and tri-substituted counterparts suggests significant differences among the structurally similar dipolar CT states. A qualitative correlation between Hammett substituent constant (σ) and the slope value from Lippert-Mataga yields a linear relationship as shown in Fig. 4, suggests that the degree of charge transfer can be correlated with the electron withdrawing strength of the acceptor units. Interestingly, a linear increase in the slope value is observed for mono-substituted derivatives whereas di- and tri-substituted TPA derivatives show the opposite trend. If the slope value is related to charge transfer interactions, molecules with larger values could have efficient charge transfer efficiency. Hence, the intriguing decrease in charge transfer efficiency or its destabilization in di- and tri-substituents having strong electron withdrawing substituent (higher σ values), would have been attributed to the moieties which are not part of the CT state.

Interestingly, **mNO_2** seems to have a specific solvent-solute effect, particularly in chlorinated solvents as shown in Fig. 3 (Figs. S3 and SI). Specifically, in chloroform and dichloromethane, **mNO_2** shows two additional shoulders at 460, and 717 nm and the peaks become broader and tailing over 800 nm. The emission in the near-infrared (NIR) region is quite exciting for a simple molecule having only TPA core. We believe that the higher energy fluorescence at 460 nm may be due to the $S_0 \leftarrow S_1$ or the local excited (LE) state. However, origin of the lowest energy fluorescence is not clear at present, and it is probably due to the charge

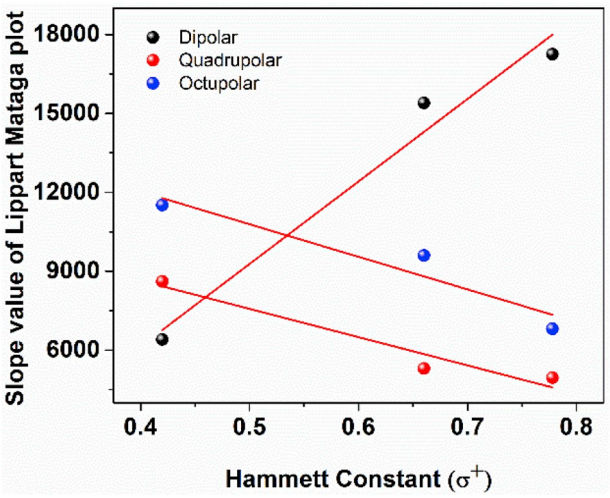

Fig. 4. A plot of Hammett constant versus slope value of the Lippert-Mataga plot of mono, di, and tri substituted TPA derivatives.

transfer interactions. The fluorescence quantum yield measurements were also carried out and the data are summarized in Tables S4, S5 and S6 (SI). All the TPA derivatives exhibit reductions in quantum yield with increasing solvent polarities, a feature generally observed for chromophores with ICT interactions.

Fluorescence decay profiles measured using time correlated single-photon counting (TSCPC) technique by using 370 nm, ~100 ps pulsed light are given in Fig. 5. The decays were fitted with exponential functions for most of the cases, however, few cases biexponential function were employed, wherein average lifetime values were used for discussion. The fluorescence lifetime of **mCN**, **mCHO**, and **mNO$_2$** in

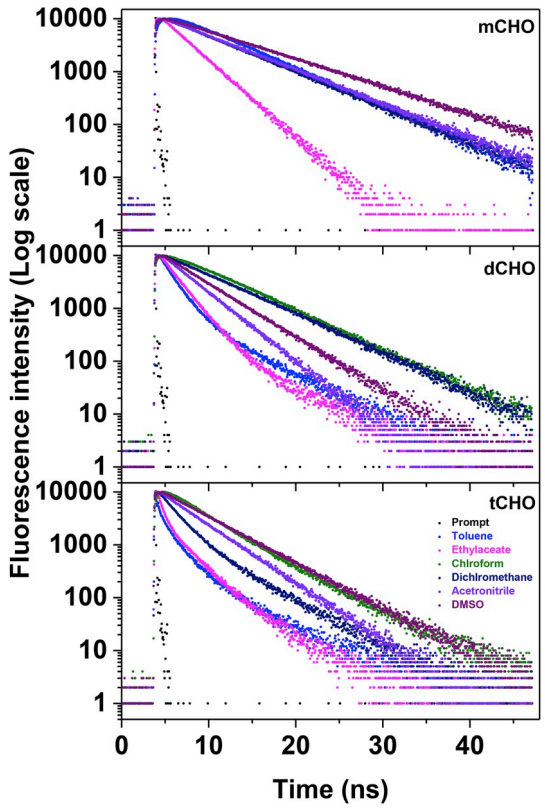

Fig. 5. Fluorescence decay profiles of **mCHO**, **dCHO** and **tCHO** in different solvents. The profiles are monitored at their respective emission maximum wavelength.

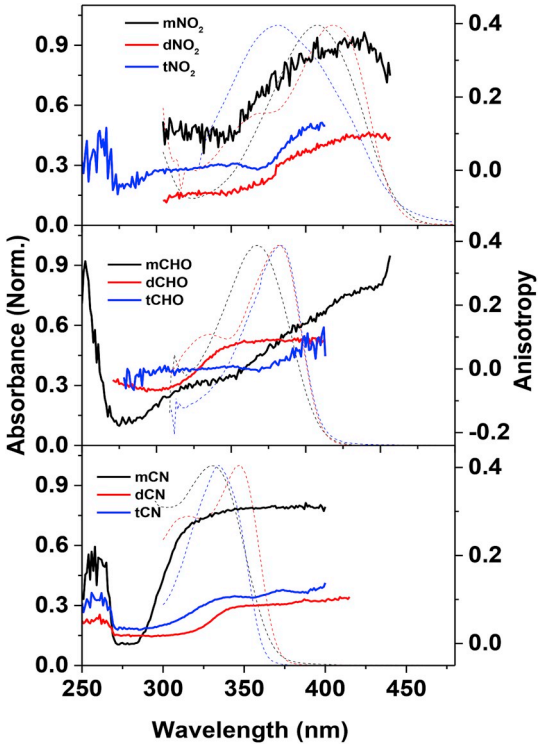

Fig. 6. Fluorescence excitation anisotropy spectra of TPA derivatives in toluene solution saturated with polystyrene beads (solid line) and dotted line represents the respective absorption spectrum.

toluene was measured to be 2.30, 0.81, and 1.10 ns respectively. Notably, the fluorescence lifetime of **mCN** and **mCHO** in acetonitrile respectively corresponds to 6.30 and 6.93 ns, which is longer by the factor of two than in toluene. The radiative ($k_r = 1/\tau_0$, where τ_0 is the natural radiative lifetime calculated using τ_F/φ_F) and non-radiative {$k_{nr} = (1-\varphi_F)/\tau_F$} rate constants calculated using the fluorescence lifetime and quantum yield are summarized Tables S4–S6 (SI). Careful examination of these values suggests that both the radiative and non-radiative rate constants are sensitive to the number and the nature of the substituents. It is possible to conclude that, though the quadrupolar and octupolar molecules form symmetry broken dipolar CT states, their lifetimes are shorter than the respective dipolar congeners in polar solvents.

To explore the nature of $S_0 \rightarrow S_n$ transitions in absorption, steady-state fluorescence excitation anisotropy measurements were carried out in highly viscous, toluene solution with polystyrene, to avoid the fast molecular rotation. Fig. 6 shows the excitation anisotropy spectra which were measured by monitoring the respective fluorescence emission maximum. In general, the anisotropy of monosubstituted TPA derivatives within the excitation spectra, i.e., $S_0 \leftarrow S_1$ transitions, corresponds to 0.35 ± 0.01, which is very close to the limiting value of 0.4, a typical value observed for the molecules having parallel excitation and emission transition dipoles. However, at higher excitation energies, the anisotropy value strongly depends on wavelength, because the absorption and emission processes involve electronic transitions with different transition-dipole orientations [39]. For the di- and tri-substituted systems, irrespective of the substituent, anisotropy value was found to be ~0.1 at lower energy excitation, which further decreases and reaches below zero at higher excitation wavelengths. The anisotropy value of 0.1 suggests that significant redistribution of excitation energy at intramolecular level among the sub-chromophoric units and also between the low and high energy excited states, prior to which the emission occurs [40,41].

Since, it has been believed that the rotation of N–C bond of amine

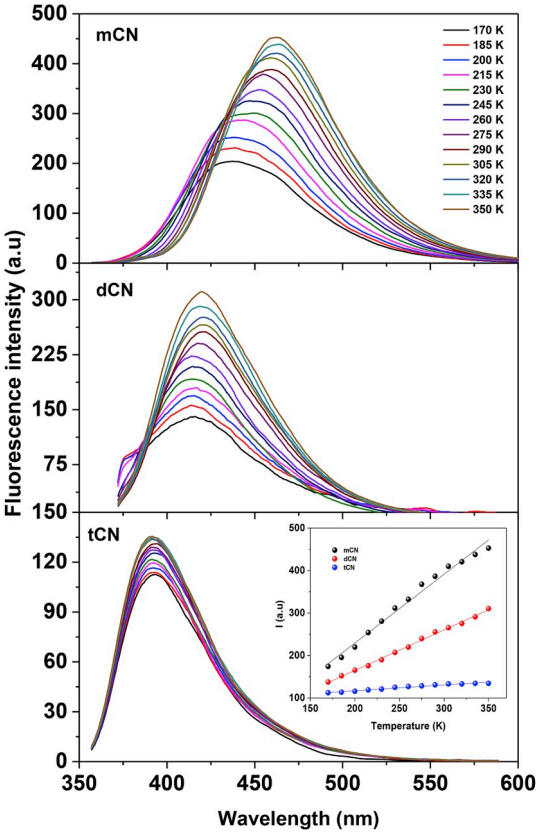

Fig. 7. Temperature-dependent fluorescence spectra of cyano-TPA derivatives in butyronitrile (BCN) solvent.

and phenyl carbon is vital in depicting the ICT interactions, controlling the rotation by lowering the surrounding temperature would impact the fluorescence properties. The fluorescence spectra of all the samples were measured between 170 and 350 K using Oxford DN cryostat in nonpolar methylcyclohexane (MCH), and polar butyronitrile (BCN) as it allows the measurements in a wider temperature range. Fluorescence intensity gradually suppressed with lowering of temperature to a different extent depending upon the solvent polarity and number of cyano groups as shown in Fig. 7 and Fig. S4. While the spectral width and maximum value appears to be relatively constant with temperature except the one for **mCN** in butyronitrile, where the emission spectrum gradually blue shifted from 462 to 436 nm with lowering of temperature from 350 K to 170 K. A plot of fluorescence intensity versus the temperature shown in Fig. 8 inset obeys the linear relationship. It has been known that only non-radiative rate constant is temperature dependent and the radiative rate constant is independent of temperature [42,43]. Lowering the temperatures resulted in rigidifying the TPA core by restricting the intramolecular rotations and vibrations around the central N–C bond, thereby hinders the processes that require the structural changes upon photoexcitation. Thus, for cyano TPA's, intensification of fluorescence while raising the temperature from cryogenic to above ambient indicates that the enhanced rotational motion and vibrations aids the fluorescence. Based on the above facts it can be concluded that the fluorescence from cyano TPA's originated from the charge transferred state with TPA and cyano respectively bearing the positive and negative charges, stiffening the N–C rotation at lower temperature that prohibits the facile orientation of the respective groups eventually affects the fluorescence intensity. A comparison of integrated fluorescence intensity in polar butyronitrile solvent reveals that nearly 1.2 fold increased fluorescence for **tCN** while that of **mCN** and **dCN** show two-fold enhancement, which suggests that more number of acceptors probably hinders the CT state formation. Interestingly, formyl and nitro TPA's renders enhanced fluorescence with lowering the temperature in both nonpolar, MCH and polar, BCN, except the nitro derivatives in BCN, which does not show measurable emission (Figure S5-S7, SI). For formyl in BCN, the fluorescence becomes enhanced by a factor of 5, 4, and 2.63 while lowering the temperature from 350 to 170 K, suggesting that the number of acceptor groups definitely play a crucial role in depicting the ICT process as witnessed from the fluorescence properties.

In general, the rate of interconversion between the two/three equivalent minimum energy geometries aided by conformational changes and solvent polarity are crucial factors in deciding the stability of symmetry broken CT state. In fact, all the minima are equally probable and hence equally populated; the observed spectra are sum of the spectra calculated as Boltzmann averages. The interconversion rate between the equivalent minima driven by the rotational motion of the N–C bond decides their stability, faster the inter-conversion and lower the stability (Figs. S8 and SI). Slowing down the rotational motion of N–C bond by lowering the temperature resulted in drastic changes in fluorescence spectra distinctly different with respect to number of acceptor groups. And signifies that dipolar CT states of quadrupolar and octupolar molecules are detrimentally affected by the acceptor moieties which are not part of the CT state.

To gain insight into the structural and electronic basis for the experimental findings, the geometry and electronic properties were calculated by using density functional theory calculations. The electron density distributions in the frontier molecular orbitals (MO) are computed to understand the ICT interactions and are shown in Figs. S9–S11 (SI). Irrespective of the substituent, electron density in the highest occupied molecular orbital (HOMO) is localized on the amino nitrogen and phenylene rings which becomes shifted to the electron deficient acceptor substituted phenylene moiety upon transition to lowest unoccupied molecular orbital (LUMO). For octupolar molecules, the electron density in LUMO is dominantly present on two of the three acceptor unit and the LUMO + 1 possess localized electron density on only one acceptor moiety. These observations underscores that all the acceptor in the TPA core are prone to be involved in the ICT interactions. In all the cases, the HOMO and LUMO becomes stabilized while going from dipolar, quadrupolar, and octupolar configuration and incidentally HOMO and HOMO-1, LUMO and LUMO + 1 are degenerate orbitals. Overall it leads to the alternations in the HOMO-LUMO energy gap and are calculated to be, 3.21, 3.16, 3.30, 3.75, 3.61, 3.67, 4.21, 4.05 and 4.10 eV for **mNO$_2$**, **dNO$_2$**, **tNO$_2$**, **mCHO**, **dCHO**, **tCHO**, **mCN**, **dCN**, and **tCN**, respectively. A plot of Hammett σ constant versus computed HOMO energy level is found to be linear (Figs. S12 and SI) but LUMO energy levels are not showing any systematic variation concerning Hammett parameter. However, slight alternations in the energy levels have been observed for different substitutions as well as with their number.

Also, natural transition orbital analysis (NTO) was performed based on the TD-DFT approach, using the optimized geometries of the excited singlet state. This method offers most compact representation of the transition density between the ground and excited states regarding an expansion into hole and electron states for each given excitation. Note that the NTO analysis is practicable only when each pair of NTOs (hole and electron) accounts for more than 90% of a transition ($\lambda > 90\%$). NTO's of the first excited singlet and ground states displayed in Fig. 8 indicates the occurrence of pronounced ICT interactions within the chromophore upon photoexcitation. The hole wave function for **mNO$_2$** and **dNO$_2$** is delocalized over the aminophenylene moiety and absent at the nitro substituted phenyl ring. On the other hand, the electron wave function of the excited S_1 state is localized on the nitro substituted phenyl ring. It indicates that upon excitation the charge is shifted from aminophenylene to nitro moiety. In the case of **tNO$_2$**, hole wave function is delocalized on the two **NO$_2$** substituted phenyl ring and electron wave function localized on the one of the **NO$_2$** substituted phenyl, as a result amino group and one of the nitro substituted phenyle ring acts as

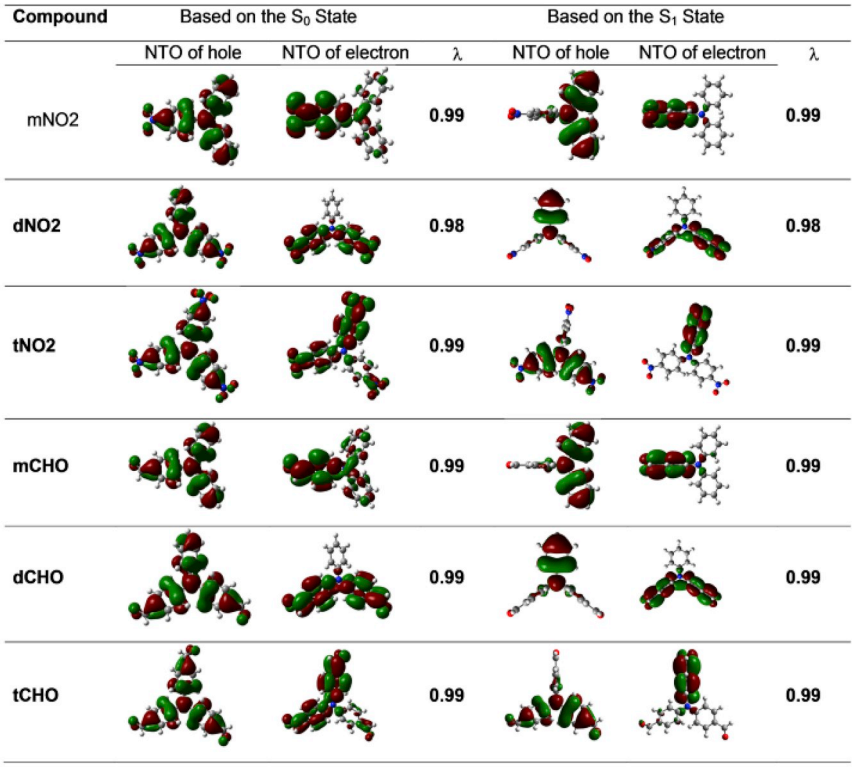

λ represents natural transition orbital eigenvalue.

Fig. 8. Contour plots of the pairs of "Natural Transition Orbitals" based on TD-DFT calculations.

an acceptor moiety and the remaining two nitro substituted phenyl rings acts as donor. The different hole-electron NTO pairs of **tNO$_2$** is due to its higher symmetry with all the phenyl ring substituted with NO_2 unit. Similar observation of the hole-electron pictures is obtained for the **mCHO**, **dCHO**, and **tCHO** systems. Franck−Condon (FC) S_1 state for all **NO$_2$** and **CHO** substituted systems is composed of average contributions (HOMO − 1 → LUMO) mainly arising delocalized transition from the aminophenylene to nitro substituted phenyl ring. It is very interesting to note that, tricyano-substituted aminophenylene (tCN) hole-electron NTOs pairs [11] are totally different from the **tNO$_2$** and **tCHO**. In the case of **tCN**, amino group and one of the cyanophenylene ring acts a donor moiety and the remaining two cyanophenylene moieties acts as an acceptor, where as in the case of **tNO$_2$** and **tCHO**, one of the nitro, CHO substituted phenyl ring acts as an acceptor moiety and the remaining two nitro and CHO substituted phenyl rings acts as donor.

Conclusions

In summary, the present work describes the intramolecular charge transfer interactions in electron rich, triphenylamine (D) substituted with the electron deficient (A) cyano, nitro, and aldehyde groups in DA, DA_2, and DA_3 configurations. The electronic properties are distinctly different with respect to the substituent as well as its number, but all the molecules show solvatochromism in fluorescence originated from the dipole moment changes upon photoexcitation. Indeed, DA_2 and DA_3 does not form $D^+(A^{\delta-})_2$ and $D^+(A^{\delta-})_3$ CT states with net zero dipole moment change identified by the non-solvatochromism in fluorescence, and forms symmetry broken, dipolar CT states, $AD^+A^-/A_2D^+A^-$ influenced by the surrounding solvent environment. Restricting the N–C bond rotation, a requisite process for the formation of ICT state by lowering the temperature below room temperature affects the fluorescence intensity though to a different extent suggest the dipolar CT states of DA_2 and DA_3 are different from their DA congeners. In addition, thus formed symmetry broken dipolar intramolecular charge transfer states of DA_2 and DA_3 derivatives seems to exhibit different dipole moment values, and excited state lifetimes concerning their respective dipolar congeners. Natural transition orbital (NTO) analysis also suggest that all the molecules exhibit intramolecular charge transfer interactions. Interestingly, the nitro substituents exhibit specific solute-solvent interactions with the chlorinated solvents, and the fluorescence spectra are trailing over visible to NIR region. The combination of emission in the NIR region with the specific solute-solvent interaction is quite intriguing and can have the potential to be used as a probe to find the chlorinated molecules. Based on the above results it can be concluded that the electronic properties of the triphenylamine derivative can be tailored by the judicious choice of substituents as well its number for optoelectronic applications.

Acknowledgements

PT acknowledges DST for INSPIRE fellowship for funding. This work was also supported by DST-Fast Track project and "TAPSUN (NWP-54)" project funded by CSIR.

Appendix A. Supplementary data

Supplementary data to this article can be found online at https://doi.org/10.1016/j.dyepig.2019.107838.

References

[1] Rumi M, Ehrlich JE, Heikal AA, Perry JW, Barlow S, Hu Z, et al. Structure−Property relationships for two-photon absorbing Chromophores: bis-donor diphenylpolyene and bis(styryl)benzene derivatives. J Am Chem Soc 2000;122(39):9500–10.
[2] Woo HY, Liu B, Kohler B, Korystov D, Mikhailovsky A, Bazan GC. Solvent effects on the two-photon absorption of distyrylbenzene chromophores. J Am Chem Soc 2005;127(42):14721–9.
[3] Terenziani F, Painelli A, Katan C, Charlot M, Blanchard-Desce M. Charge instability

in quadrupolar Chromophores: symmetry breaking and solvatochromism. J Am Chem Soc 2006;128(49):15742–55.
[4] Carlotti B, Benassi E, Fortuna CG, Barone V, Spalletti A, Elisei F. Efficient excited-state symmetry breaking in a cationic quadrupolar system bearing diphenylamino donors. ChemPhysChem 2016;17(1):136–46.
[5] Dozova N, Ventelon L, Clermont G, Blanchard-Desce M, Plaza P. Excited-state symmetry breaking of linear quadrupolar chromophores: a transient absorption study. Chem Phys Lett 2016;664(Supplement C):56–62.
[6] Kim W, Sung J, Grzybowski M, Gryko DT, Kim D. Modulation of symmetry-breaking intramolecular charge-transfer dynamics assisted by pendant side chains in π-linkers in quadrupolar diketopyrrolopyrrole derivatives. J Phys Chem Lett 2016;7(15):3060–6.
[7] Dereka B, Rosspeintner A, Krzeszewski M, Gryko DT, Vauthey E. Symmetry-breaking charge transfer and hydrogen bonding: toward asymmetrical photochemistry. Angew Chem Int Ed 2016;55(50):15624–8.
[8] Balasaravanan R, Sadhasivam V, Siva A, Pandi M, Thanasekaran G, Arulvasu C. Synthesis, characterization and photophysical studies of D-π-A based conjugated triphenylamine derivatives. Chemistry Select 2016;1(11):2792–801.
[9] Li Y, Zhou M, Niu Y, Guo Q, Xia A. Solvent-dependent intramolecular charge transfer delocalization/localization in multibranched push-pull chromophores. J Phys Chem Lett 2015;143(3). 034309-12.
[10] Seintis K, Agathangelou D, Cvejn D, Almonasy N, Bures F, Giannetas V, et al. Femtosecond to nanosecond studies of octupolar molecules and their quadrupolar and dipolar analogues. Phys Chem Chem Phys 2017;19(25):16485–97.
[11] Easwaramoorthi S, Thamaraiselvi P, Duraimurugan K, Beneto AJ, Siva A, Nair BU. Charge instability of symmetry broken dipolar states in quadrupolar and octupolar triphenylamine derivatives. Chem Commun 2014;50(52):6902–5.
[12] Jiménez-Sánchez A, Isunza-Manrique I, Ramos-Ortiz G, Rodríguez-Romero J, Farfán N, Santillan R. Strong dipolar effects on an octupolar luminiscent chromophore: implications on their linear and nonlinear optical properties. J Phys Chem A 2016;120(25):4314–24.
[13] Poronik YM, Hugues V, Blanchard-Desce M, Gryko DT. Octupolar merocyanine dyes: a new class of nonlinear optical chromophores. Chem Eur J 2012;18(30):9258–66.
[14] Whitby R, Ben-Tal Y, MacMillan R, Janssens S, Raymond S, Clarke D, et al. Photoinitiators for two-photon polymerisation: effect of branching and viscosity on polymerisation thresholds. RSC Adv 2017;7(22):13232–9.
[15] Pawlicki M, Collins HA, Denning RG, Anderson HL. Two-photon absorption and the design of two-photon dyes. Angew Chem Int Ed 2009;48(18):3244–66.
[16] Wang J, Liu K, Ma L, Zhan X. Triarylamine: versatile platform for organic, dye-sensitized, and perovskite solar cells. Chem Rev 2016;116(23):14675–725.
[17] Liang M, Chen J. Arylamine organic dyes for dye-sensitized solar cells. Chem Soc Rev 2013;42(8):3453–88.
[18] Yang C-H, Chen H-L, Chuang Y-Y, Wu C-G, Chen C-P, Liao S-H, et al. Characteristics of triphenylamine-based dyes with multiple acceptors in application of dye-sensitized solar cells. J Power Sources 2009;188(2):627–34.
[19] Tydlitát J, Achelle S, Rodríguez-López J, Pytela O, Mikýsek T, Cabon N, et al. Photophysical properties of acid-responsive triphenylamine derivatives bearing pyridine fragments: towards white light emission. Dyes Pigments 2017;146(Supplement C):467–78.
[20] Agarwala P, Kabra D. A review on triphenylamine (TPA) based organic hole transport materials (HTMs) for dye sensitized solar cells (DSSCs) and perovskite solar cells (PSCs): evolution and molecular engineering. J Mater Chem 2017;5(4):1348–73.
[21] Gudeika D, Michaleviciute A, Grazulevicius JV, Lygaitis R, Grigalevicius S, Jankauskas V, et al. Structure properties relationship of donor–acceptor derivatives of triphenylamine and 1,8-naphthalimide. J Phys Chem C 2012;116(28):14811–9.
[22] Duraimurugan K, Balasaravanan R, Siva A. Electron rich triphenylamine derivatives (D-π-D) for selective sensing of picric acid in aqueous media. Sens Actuators B Chem 2016;231(Supplement C):302–12.
[23] Parthasarathy V, Fery-Forgues S, Campioli E, Recher G, Terenziani F, Blanchard-Desce M. Dipolar versus octupolar triphenylamine-based fluorescent organic nanoparticles as brilliant one- and two-photon emitters for (Bio)imaging. Small 2011;7(22):3219–29.
[24] Dumat B, Bordeau G, Aranda AI, Mahuteau-Betzer F, Harfouch YE, Metge G, et al. Vinyl-triphenylamine dyes, a new family of switchable fluorescent probes for targeted two-photon cellular imaging: from DNA to protein labeling. Org Biomol Chem 2012;10(30):6054–61.
[25] Kumar S, Singh P, Kumar P, Srivastava R, Pal SK, Ghosh S. Exploring an emissive charge transfer process in zero-twist donor–acceptor molecular design as a dual-state emitter. J Phys Chem C 2016;120(23):12723–33.
[26] Larsen CB, van der Salm H, Shillito GE, Lucas NT, Gordon KC. Tuning the rainbow: systematic modulation of donor–acceptor systems through donor substituents and solvent. Inorg Chem 2016;55(17):8446–58.
[27] Larsen CB, Barnsley JE, van der Salm H, Fraser MG, Lucas NT, Gordon KC. Synthesis and optical properties of unsymmetrically substituted triarylamine hexaaza-trinaphthalenes. Eur J Org Chem 2017;2017(17):2432–40.
[28] Nemkovich NA, Detert H, Schmitt V. Structural symmetry breaking in octupolar tetrastyrylpyrazines and their dipole moments in equilibrium ground and Franck-Condon excited state. J Photochem Photobiol A Chem 2018;354:139–46.
[29] Dereka B, Rosspeintner A, Li Z, Liska R, Vauthey E. Direct visualization of excited-state symmetry breaking using ultrafast time-resolved infrared spectroscopy. J Am Chem Soc 2016;138(13):4643–9.
[30] Song J, Jang SY, Yamaguchi S, Sankar J, Hiroto S, Aratani N, et al. 2,5-Thienylene-Bridged triangular and linear porphyrin trimers. Angew Chem Int Ed 2008;47(32):6004–7.
[31] Wu X, Dube MA, Fry AJ. Electrophilic nitration of triphenylamines as a route to high oxidation potential electrocatalysts. Polynitration, nitrodebromination, and bromine dance. Tetrahedron Lett 2006;47(44):7667–9.
[32] Mallegol T, Gmouh S, Meziane MAA, Blanchard-Desce M, Mongin O. Practical and efficient synthesis of tris(4-formylphenyl)amine, a key building block in materials chemistry. Synthesis 2005 2005;11:1771–4.
[33] Gaifa Lai XRB, Santos Javier, Eric A. Reinvestigation of the Vilsmeier-Haack formylation of triphenylamine. Mintz Synlett 1997;11:1275–6.
[34] Brown GM, Freeman GR, Walter RI. Crystal structure of tri(p-biphenylyl)aminium perchlorate. J Am Chem Soc 1977;99(21):6910–5.
[35] Tang Xianglin, Liu Weimin, Wu Jiasheng, Lee Chun-Sing, Juanjuan You a, Wang P. J Org Chem 2010;75:7273–8.
[36] Hilger Anouk, Gisselbrecht Jean-Paul, Tykwinski Rik R, Boudon Corinne, Schreiber Martin, Martin Rainer E, et al. J Am Chem Soc 1997;119:2069–78.
[37] Frisch GWT MJ, Schlegel HB, Scuseria GE, Robb MA, Cheeseman JR, Scalmani G, Barone V, Mennucci B, Petersson GA, Nakatsuji H, Caricato M, Li X, Hratchian HP, Izmaylov AF, Bloino J, Zheng G, Sonnenberg JL, Hada M, Ehara M, Toyota K, Fukuda R, Hasegawa J, Ishida M, Nakajima T, Honda Y, Kitao O, Nakai H, Vreven T, Montgomery Jr. JA, Peralta JE, Ogliaro F, Bearpark M, Heyd JJ, Brothers E, Kudin KN, Staroverov VN, Keith T, Kobayashi R, Normand J, Raghavachari K, Rendell A, Burant JC, Iyengar SS, Tomasi J, Cossi M, Rega N, Millam JM, Klene M, Knox JE, Cross JB, Bakken V, Adamo C, Jaramillo J, Gomperts R, Stratmann RE, Yazyev O, Austin AJ, Cammi R, Pomelli C, Ochterski JW, Martin RL, Morokuma K, Zakrzewski VG, Voth GA, Salvador P, Dannenberg JJ, Dapprich S, Daniels AD, Farkas O, Foresman JB, Ortiz JV, Cioslowski J, Fox DJ. Gaussian 09, revision C01. Wallingford CT: Gaussian, Inc; 2010.
[38] Hansch C, Leo A, Taft RW. A survey of Hammett substituent constants and resonance and field parameters. Chem Rev 1991;91(2):165–95.
[39] Dvořák M, Michl M, Almonasy N, Nepraš M, Ladd N, Fidler V. Fluorescence anisotropy of branched molecules containing 1-aminopyrene chromophores. J Fluoresc 2011;21(3):971–4.
[40] MvdA Verbouwe, De Schryver FC, Piet JJ, Warman JM. J Am Chem Soc 1998;120:1319–24.
[41] Hall RD, Valeur B, Weber G. Polarization of the fluorescence of triphenylene. A planar molecule with three-fold symmetry. Chem Phys Lett 1985;116(2):202–5.
[42] Birks JB. Photophysics of aromatic molecules. London; New York: Wiley-Interscience; 1970.
[43] Turro NJ. Modern molecular photochemistry. Menlo Park, Calif: Benjamin/Cummings Pub. Co; 1978.